Passive 5.8-GHz Radio-Frequency Identification Tag for Monitoring Oil Drill Pipe

Berndie Strassner, *Student Member, IEEE*, and Kai Chang, *Fellow, IEEE*

***Abstract*—This paper reports a new passive 5.8-GHz radio-frequency identification tag proposed for monitoring oil drill pipe (patent pending). The tag is to be inserted into the tool joint of the drill pipe in order to predict the pipe's lifetime and to provide inventory control. The tag requires a minimal incident power density of 13.5 mW/cm^2 to establish a link and transmit 64-bit coded information to the interrogating reader. The tag uses a circular patch etched on a 60-mil Duroid with $\varepsilon_r = 2.33$ to receive the interrogating RF power and transmit the identification (ID) information simultaneously. An efficient Schottky diode is used to rectify the RF power to provide the dc power necessary to operate the "on-board" electronics. A p-i-n diode modulates the tag's ID code onto the 5.8-GHz carrier frequency. The tag's physical size has to be small so that it can be imbedded into the pipe without weakening the structure. It has been designed to withstand large pressures normal to its surface. The system was successfully demonstrated in the laboratory.**

***Index Terms*—Microwave systems, passive tags, radio-frequency identification (RFID), rectifying antenna.**

I. Introduction

RADIO-FREQUENCY identification (RFID) systems are used for identifying and tracking objects as in the case of automobile tolling [1], collision avoidance [2], and security systems [3]. Other applications include baggage tracking in airports [4], [5], land-mine detection [6], and even identifying sea mammals [7], but its benefit to the oil industry has not been fully explored [8]. Most RFID systems consist of a reader and tag. The reader transmits power to the tag, which then sends a coded signal back to the reader [9], [10]. For oil drill-pipe monitoring, this coded signal contains information about the drill pipe being used including the drill-pipe identification (ID), size, and previous usage. The RFID tag will provide automatic tracking of both the up and down and rotational movement of the drill pipe. With this information, someone monitoring the drill pipe can determine its cumulative use and when it needs to be replaced. Drilling holes for tapping oil reserves is a costly and complex undertaking. When a drill pipe is overused and breaks in the ground, the hole leading to the oil supply, which is now blocked by the broken drill pipe, must be abandoned. This is a very costly problem, especially for offshore operations, because a new hole must be drilled, which can reach depths of over 15 000 ft. To avoid these pipe failures, drill pipe is presently being replaced after approximately 25% of its lifetime has elapsed. Better inventory and usage control will enable the pipes to be used for longer periods of time, i.e., 75% of their lifetimes, resulting in huge cost savings for oil-drilling companies.

The idea of placing an RFID tag on the drill pipe for monitoring purposes has been around for over a decade now [11]. The tags presently used operate in the kilohertz range and have read ranges on the order of an inch. These short read ranges are due to the low gain loop antennas that serve to receive and transmit the energy. The reader must also pass the tag at a slow velocity due to the slow data rate that is directly dependent upon the frequency of operation. Due to the short read range and the slow data rate, the drilling is shut down in order to accurately read the tag. The cost of shutting down operations for reading the tag and then to restart the drilling process is approximately $30 000. These costs can quickly escalate, justifying the need for a way to efficiently monitor the drill pipe's history as it is operating.

The reader interrogates the tag whenever the tag leaves the "down hole" environment and rises above the earth's surface. The "down hole" environment that the tag invades is extremely harsh. Temperature can reach 230 °C and the outside pressures normal to the tag's surface can exceed 20 000 lbf/in^2. Most RFID systems use batteries to drive their "on-board" electronics. However, at these high storage temperatures, batteries often fail. An alternative for powering the tag's electronics is to use rectifying circuits that convert microwave energy into dc energy. Rectifying circuits are instrumental in rectifying antennas [12], [13] and "passive" RFID applications [14], [15]. This rectification is achieved when microwave energy is incident upon a Schottky detector diode. The Schottky diode, through a mixing process, converts a large percentage of the microwave energy into dc power. The rectified or dc portion of the energy is then used to power the electronics that create the tag's unique ID. Since no battery is present, the tag is referred to as a "passive" RFID tag.

While most existing microwave RFID technologies are designed at 2.45 GHz [16], [17], the system being proposed is a passive system operating at 5.8 GHz. This frequency is chosen because it is a industrial–scientific–medical (ISM) band, but mainly because of size restrictions on the tag. The tag must fit in a cylinder 0.75-in tall and 1 in in diameter. This size restriction is due to the rotational stresses on the oil drill pipe. If too large a tag is used, the structural integrity of the pipe's high-grade steel is compromised, which could lead to the pipe twisting into multiple pieces. The smaller tag also has the advantage of having

Manuscript received December 19, 2001; revised July 29, 2002. This work was supported by the State of Texas and by Texas A&M University.

B. Strassner was with the Department of Electrical Engineering, Texas A&M University, College Station, TX 77843-3128 USA. He is now with Sandia National Laboratories, Albuquerque, NM 87185-0529 USA.

K. Chang is with the Department of Electrical Engineering, Texas A&M University, College Station, TX 77843-3128 USA.

Digital Object Identifier 10.1109/TMTT.2002.807832

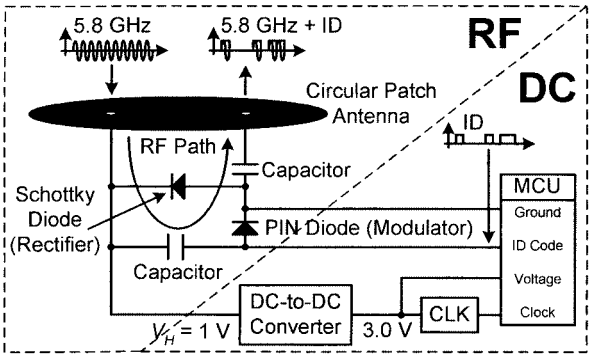

Fig. 1. RFID tag circuit block diagram. RF and dc represent the microwave and digital portions, respectively. The voltage V_H is the rectified voltage from the Schottky diode.

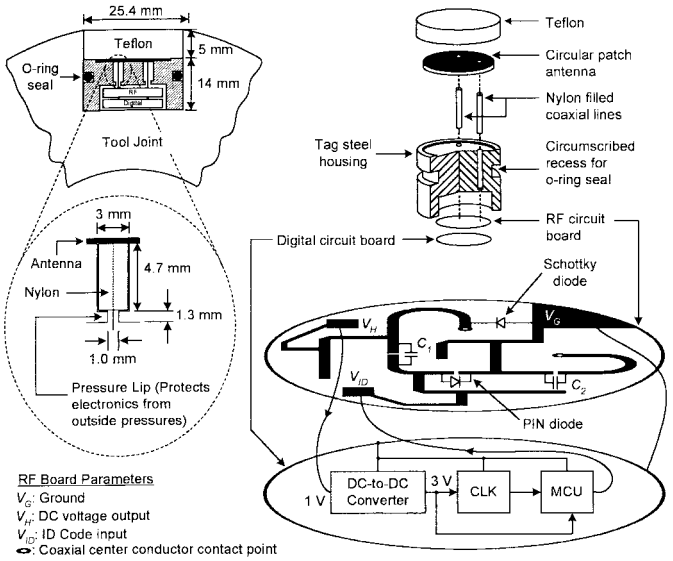

Fig. 2. Tag recess and 3-D structure view.

less force normal to its surface. The tag's structure must be designed to isolate the outside 20 000 psi pressure from reaching the sensitive electronics.

The last obstacle to designing the tag for drill-pipe monitoring is the presence of drill mud on the pipe's surface during interrogation. This mud functions as a drill bit lubricant and transport of rock and materials from the drilling location to the earth's surface. The reader interrogates the tag when the pipe surfaces. At this time, a thin film of drill mud may be present on the pipe's surface. The reader/tag link must be able to penetrate this thin wet mud layer. Many ideas of how to reduce the mud on the tag such as water and air jets are being considered. The design presented will address some of these problem issues associated with real-time drill-pipe monitoring.

II. Operational Theory and Component Design

A block diagram of the tag is shown in Fig. 1. The tag consists of both an RF section and a digital section denoted by dc. The reader interrogates the tag using a continuous wave (CW) of energy at 5.8 GHz. The tag then simultaneously returns its ID modulated on the 5.8-GHz carrier back to the reader.

A. Tag System Components

The tag's placement in the tool joint of the drill pipe and the interior of the tag are presented in Fig. 2. The tool joint is a junction at which two drill pipes are connected. Generally, this junction is larger in diameter than the remaining pipe. The larger diameter allows for greater structural integrity for placing the tag than elsewhere along the drill pipe. The tag is recessed 19 mm ($\sim$0.75 in) into the tool joint of the drill pipe. A 5-mm ($\sim$0.25 in)-thick Teflon cover is then placed over the tag in order to protect the tag from the "down-hole" environment. This Teflon "puck" is large enough in diameter so that, when it is forced into the tool joint, it forms a hermetic seal. The Teflon's inherent slick surface also helps to clear the drill mud from the surface of the tag. The circular patch located behind the Teflon couples RF power in and out of the tag. The patch has two ports that are orthogonally spaced [18] on its surface 4.5 mm away from the patch's center. The patch is linearly polarized with one port being H-plane polarized and the other E-plane polarized. These orthogonal ports are also isolated and, thus, can perform receive and transmit functions simultaneously.

The patch is connected to the RF circuitry by two Nylon-filled coaxial lines. These coaxial lines have a cross-sectional area of 7.1 mm^2. Assuming the 20 000-lbf/in^2 exterior pressure is uninhibited by the Teflon or the antenna, 220 lb of force will be applied to each of the Nylon coaxial lines. The Nylon maintains its rigidity at this force so as to not change the electromagnetic properties of the coaxial lines. The short lip section between the Nylon coaxial lines and diodes keeps the pressure on the tag's Teflon surface from reaching the RF and digital circuit boards.

After the 5.8-GHz energy is collected by the patch antenna, it flows down the coaxial line leading to the Metellics MSS30-142-E20 Schottky rectifying diode depicted in Figs. 1 and 2. This diode then converts a major portion of the microwave energy into dc power consisting of voltage V_H. The remaining power is distributed at 5.8 GHz and its higher order harmonic frequencies. This rectification is responsible for making the tag passive since it generates the dc power that operates all of the "on-board" electronics. A dc-to-dc converter is then used to step up the rectified dc voltage in order to lower the Schottky's rectification requirement, which ultimately lowers the transmit power necessary to turn-on the tag's electronics. The converter used is a MC33466H-30KT1 manufactured by Motorola. It uses a 1-V input to produce a 3-V output. The converter's 3-V output drives both the 16-MHz clock oscillator and the Motorola MC68HC908JK3-CDW microcontroller. The microcontroller produces a 64-bit ID unique to the tag and is programmed to repeat the code until it shuts down due to a lack of turn-on voltage. This repeating 64-bit ID sequence of 1 s (3 V) and 0 s (0 V) is used to modulate the 5.8-GHz energy remaining from the Schottky diode mixing process. This 5.8-GHz energy that arose from the Schottky diode travels through the low-loss capacitor C_1 and couples to a MA/COM 4P804-129 p-i-n diode. When $V_{\rm ID} = 3$ V, this p-i-n diode shorts and allows the 5.8-GHz energy to pass through it. Conversely, in the case where $V_{\rm ID} = 0$ V, the p-i-n open-circuits to reflect the 5.8-GHz energy back to the Schottky diode where it remixes and creates more dc power. Thus, the p-i-n diode functions as a switch [19] to modulate

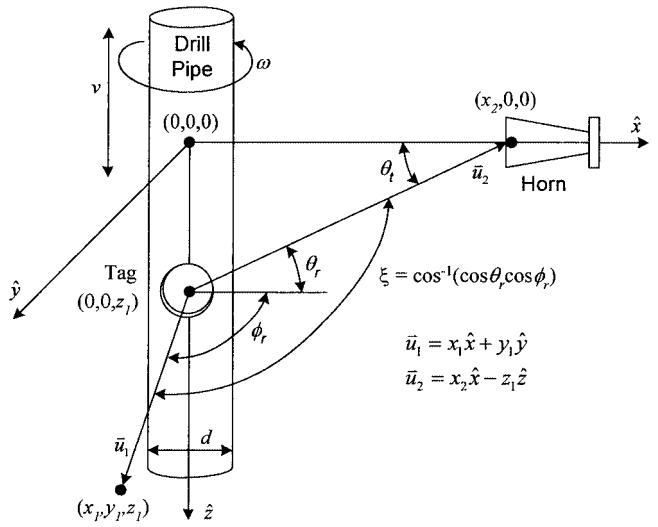

Fig. 3. 3-D spatial orientation of the tag with respect to the reader's horn antenna. The horn antenna is fixed at the point (x_2, 0, 0) and the tag rotates about and moves vertically along the z-axis. The vector $\vec{u}_1$ is normal to the tag's surface and represents the tag's broadside orientation. The tag is inserted into the tool joint such that the tag's patch antenna has a broadside orientation in the direction of (x_1, y_1, z_1).

the ID code on the 5.8-GHz carrier frequency. The modulated signal then travels through another low-loss capacitor C_2 to reach the connection to the coaxial line. The coaxial line is connected to the patch antenna where it radiates back to the reader. Both low-loss capacitors are required to separate the three voltage levels, i.e., ground, high, and the ID code. At the locations of these three voltage levels are three $\lambda/4$ wavelength stubs that are used as RF chokes to isolate the microwave energy from the digital circuitry. The 64-bit ID sequence has 2^{64} or 1.8×10^{19} different code combinations with which to ID the drill pipe. Each year approximately 400 000 new drill pipes are manufactured. Thus, there exits enough unique code sequences to identify all newly manufactured drill pipes for the foreseeable future.

B. Tag/Reader Link

In order to determine the transmit power necessary to operate the tag, a mathematical analysis of the tag/reader link is formulated. Fig. 3 presents a three-dimensional (3-D) view of the tag's orientation with respect to the reader's horn antenna. The reader's horn antenna is located along the $\hat{x}$-axis. The tag has been placed along the $\hat{z}$-axis. Assuming $x_2 \gg d/2$ where the diameter of the drill pipe is represented by d, and the horizontal distance between the horn antenna and the tag located on the drill pipe is x_2, the ratio of the power received by the tag to the power transmitted by the reader is given by the Friis transmission equation [20] as

$$\frac{P_r}{P_t} = \left(\frac{\lambda_o}{4\pi|\vec{u}_2|}\right)^2 G_t(\theta_t, \phi_t) G_r(\theta_r, \phi_r) \left|\hat{\rho}_t \cdot \hat{\rho}_r^*\right|^2 \quad (1)$$

where P_r and P_t are the received and transmitted power, respectively. The length $|\vec{u}_2|$ represents the distance between the horn and tag's circular patch antenna. The free-space wavelength λ_o of the 5.8-GHz energy is 5.17 cm. The gains of the reader and tag antennas for an arbitrary orientation are represented by $G_t(\theta_t, \phi_t)$ and $G_r(\theta_r, \phi_r)$, where θ_t, θ_r, ϕ_t, and ϕ_r are in degrees. Fig. 3 shows that $\theta_t = \theta_r$. The quantity $|\hat{\rho}_t \cdot \hat{\rho}_r^*|$ stands for the polarization mismatch and is assumed to be unity since both antennas are linearly polarized and well aligned. The tag rotates about the $\hat{z}$-axis at an angular speed ω and moves vertically along the $\hat{z}$-axis at a vertical speed v. Contrarily, the reader's horn antenna is held fixed so that it always faces the $\hat{z}$-axis. Thus, the horn has no ϕ dependence, only θ dependence, and (1) becomes

$$\frac{P_r}{P_t} = \left(\frac{\lambda_o}{4\pi\sqrt{x_2^2 + z_1^2}}\right)^2 G_t(\theta_r) G_r(\theta_r, \phi_r) \quad (2)$$

where the distance z_1 represents the tag's vertical displacement from the origin.

From Fig. 3, it can be shown that the angle ξ between the line-of-sight vector $\vec{u}_2$ connecting the tag and reader and the normal vector $\vec{u}_1$ of the tag's antenna is found from the dot product between the two vectors as

$$\xi = \cos^{-1}\left(\frac{\vec{u}_1 \cdot \vec{u}_2}{|\vec{u}_1||\vec{u}_2|}\right) = \cos^{-1}\left(\frac{x_1 x_2}{\sqrt{x_1^2 + y_1^2}\sqrt{x_2^2 + z_1^2}}\right). \quad (3)$$

It can also be shown that $\tan\phi_r = y_1/x_1$ and $\tan\theta_r = z_1/x_2$. Using these two equations and the trigonometric identity $1 + \tan^2 a = \sec^2 a = 1/\cos^2 a$, (3) reduces to

$$\begin{aligned}\xi &= \cos^{-1}\left(\frac{x_1 x_2}{\sqrt{x_1^2 + x_1^2\tan^2\phi_r}\sqrt{x_2^2 + x_2^2\tan^2\theta_r}}\right) \\ &= \cos^{-1}(\cos\phi_r \cos\theta_r). \end{aligned} \quad (4)$$

The gain of the tag $G_r(\theta_r, \phi_r)$ can now be expressed in terms of the single variable ξ as $G_r(\xi)$. Therefore, given z_1, x_2, θ_r, and ϕ_r, one can calculate P_r in terms of P_t.

C. Data Rate

The data rate is chosen based on the interrogation time experienced by the tag. This interrogation time has been chosen to be the time in which the tag located at point (0, 0, z_1) appears within the 3-dB beamwidth of the reader's horn antenna located at (x_2, 0, 0). To complete this transmit/receive link, a clock speed for the data must be chosen based upon the interrogation time, which is a function of both the rotational angular velocity ω and ascent/descent velocity v. Two cases for determining the interrogation time are analyzed here. The first case looks solely at the pipe's vertical movement in the $\hat{x}$–$\hat{z}$-plane when $\phi_r = 0°$, and the second looks at the rotational movement in the $\hat{x}$–$\hat{y}$-plane when $\theta_r = 0°$. The separation of the vertical and rotational components allows for an easy determination of the approximate digital clocking necessary to communicate multiple data reads between the reader and tag as the tag passes the horn antenna.

For the first case, the length between the tag and reader's transmit horn is x_2. The time that elapses during the tag's vertical movement from $-z_1\hat{z}$ to $z_1\hat{z}$ in terms of the angle θ_r is

$$t_1 = \frac{2z_1}{v} = \frac{2x_2}{v}\tan(\theta_r) \quad (5)$$

where v represents the vertical speed of the tag.

For the second case, the angular rotational velocity ω of the drill pipe is taken into account. The angle between the normal vectors of both the tag's circular patch and reader horn antenna is represented by ϕ_r. The time that elapses during the tag's rotation for which its normal vector sweeps from the point (x_1, $-y_1$, 0) to the point (x_1, y_1, 0) is

$$t_2 = \frac{2\phi_r}{\omega}. \tag{6}$$

For determining the interrogation time of the tag, the 40° 3-dB E- and H-plane beamwidths of the reader's horn antenna are inputted into (5) and (6) as $2\theta_r$ and $2\phi_r$, respectively. The horn's 3-dB beamwidths are used since they are narrower than the 75° orthogonal beamwidths of the tag's patch antenna. For most drilling operations, the distance x_2 between the tag and reader's horn antenna is 1.0 ft (30.5 cm). For this distance and given that the vertical drill-pipe velocity $v = 8.8$ ft/s $= 268.2$ cm/s and the angular rotational velocity $\omega = 350$ rev/min $= 5.833$ rev/s $= 36.652$ rad/s, $t_1 = 82.8$ ms, and $t_2 = 19.1$ ms. The smaller time t_2 determines the number of reads during interrogation depending upon the number of bits n_b in each read. Since t_2 is always the shorter time for the given ω and v, the number of reads n_r is represented by

$$n_r = \frac{f_{\mathrm{CLK}} \cdot t_2}{n_b} \tag{7}$$

where f_{CLK} represents the frequency of the clock used for the tag's ID sequence. The crystal oscillator denoted as CLK in Fig. 2 operates at 16 MHz. However, the microcontroller slows this down to 33.3 kHz in order to view the sequence on an oscilloscope. This 33.3-kHz clock rate is the data rate f_{CLK}. If the drill pipe uses 64-bit ID and $t_2 = 19.1$ ms, the number of reads $n_r = 10$. More reads means better data correction for averaging out erroneous bits.

The frequency 5.8 GHz is chosen primarily on the size limitation of the antenna. However, this frequency also provides enough carrier oscillations in each information bit to provide detectable information at the reader. The period of the clock is $T_{\mathrm{CLK}} = 1/f_{\mathrm{CLK}} = 30$ μs. Similarly, the period of the carrier frequency 5.8 GHz is $T_{\mathrm{RF}} = 172.4$ ps. Therefore, the number of carrier oscillations n_o in a single clock cycle is

$$n_o = \frac{T_{\mathrm{CLK}}}{T_{\mathrm{RF}}} \tag{8}$$

or 174 thousand cycles. If T_{RF} is on the order of or less than T_{CLK}, the data will not transmit correctly. If more reads are necessary for better error correction, the clock frequency can be increased. The CW energy at 5.8 GHz provides plenty of oscillations on the 33.3-kHz ID to produce a clean distinguishable modulated ID sequence. Thus, the tag's vertical and rotational movements do not create any data rate complications in providing a link between the reader and tag at 5.8 GHz.

III. Measured Data for RFID Tag

A. Circular Patch Antenna

The return loss and port isolation for the circular patch antenna with no recess and no Teflon cover is shown in Fig. 4. The ports are orthogonally spaced 4.5 mm from the center of the patch, and the patch's diameter is 17.5 mm. With no Teflon cover, the patch has a resonant frequency of 6.04 GHz. The orthogonal ports are isolated by over 20 dB from 5.6 to 6.4 GHz. This isolation makes it possible for the tag to receive E-plane and transmit H-plane or vice versa with minimal crosstalk between the ports.

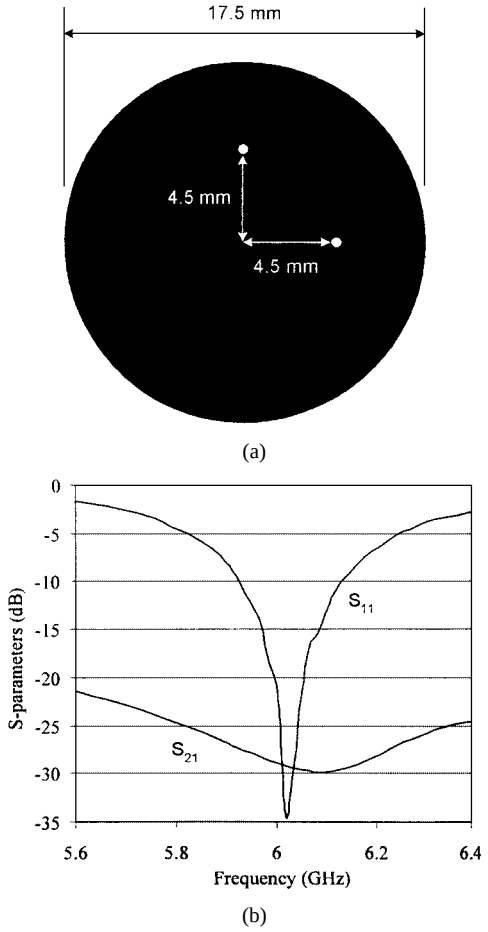

Fig. 4. Circular patch dimensions and S-parameters with no recess or Teflon cover. $S21$ reveals the >20-dB isolation between the orthogonally spaced ports. The circular patch is etched on Duroid 5870 with $\varepsilon_r = 2.33$ and a thickness of 1.524 mm.

As the Teflon cover thickness is increased, the tag's center resonant frequency decreases, as shown in Fig. 5. When the drilling pipe is manufactured, the tag is recessed and covered with a 5-mm Teflon cover. The resonant frequency for the 5-mm cover is 5.74 GHz. As the pipe is used and worn down, its diameter d decreases. This causes the Teflon thickness t to also decrease from the initial 5 to 3 mm. When the Teflon thickness reaches 3 mm, the pipe must be replaced due to its decrease in diameter in order to avoid failure down hole. At this point, the resonant frequency has shifted up to 5.82 GHz. This shift in resonant frequency could also be used to determine when a pipe's diameter has been worn down enough to warrant replacement.

The E- and H-plane patterns for both the horn and patch antenna are shown in Fig. 6. The horn and patch have 5.8-GHz broadside gains of 15.3 and 8 dB, respectively. Their polynomial gain approximations $\Psi_t(\theta_r)$ and $\Psi_r(\xi)$ are shown in Fig. 6 and are used to compute the horn and patch gains at any angle as

$$G_t(\theta_r) = 10^{\psi_t(\theta_r)/10} = 10^{(-0.0124\theta_r^2 + 0.001\theta_r + 15.3/10)} \tag{9}$$

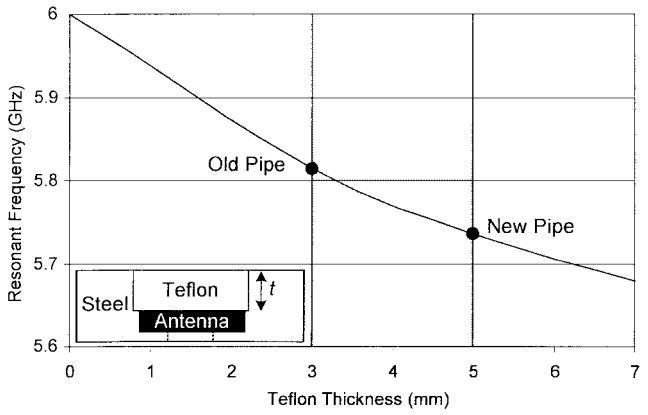

Fig. 5. Tag resonant frequency versus Teflon thickness t. New drill pipe will have a Teflon thickness of 5 mm. When the Teflon wears to a thickness of 3 mm, the pipe needs to be replaced.

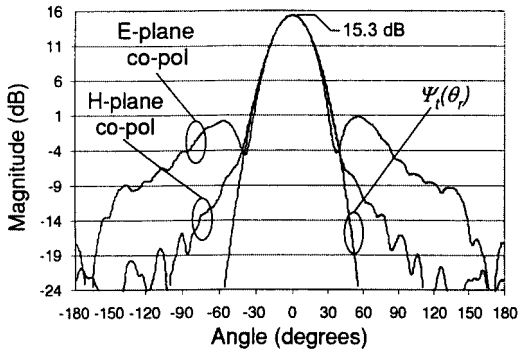

(a)

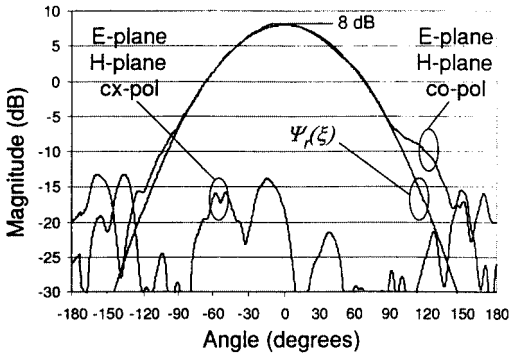

(b)

Fig. 6. (a) Chart shows the E- and H-plane patterns for the standard gain horn antenna with polynomial approximation $\Psi_t(\theta_r)$ in decibels. This approximation is good for $-30^\circ < \theta_t < 30^\circ$. (b) Chart shows the E- and H-plane patterns for the tag's circular patch antenna with polynomial approximation $\Psi_r(\xi)$ in decibels. This approximation is good for $-90^\circ < \xi < 90^\circ$. All angles are measured off broadside.

and

$$G_r(\xi) = 10^{\psi_r(\xi)/10} = 10^{(-0.0018\xi^2 + 0.0032\xi + 8/10)}. \quad (10)$$

By inserting (9) and (10) into (2), it is possible to predict the power received by the tag depending on its orientation with respect to the reader.

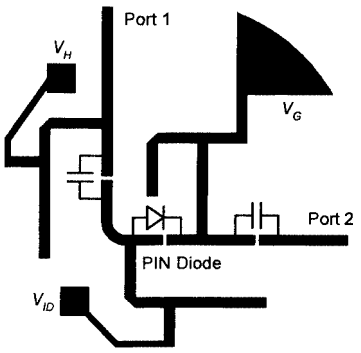

(a)

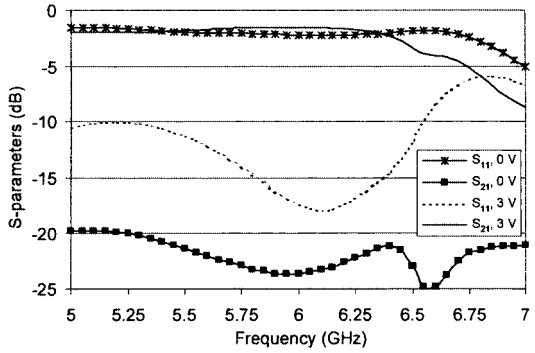

(b)

Fig. 7. Measured p-i-n diode modulation for both on and off states of the diode. For the on state, $V_{\rm ID} - V_G = 3$ V. Similarly, the off state occurs when $V_{\rm ID} - V_G = 0$ V. The RF circuit is etched on a Duroid 6010.8 with $\varepsilon_r = 10.8$ and a thickness of 0.635 mm.

B. p-i-n Diode Modulation Circuit Performance

The S-parameters for the p-i-n diode modulation circuit are shown in Fig. 7. The circuit consists of three $\lambda_g/4$ stubs at 5.8 GHz, which act as RF chokes to isolate the RF energy from the electronics. Two 0603 3A102K dc-blocking capacitors manufactured by the AVX Corporation, Myrtle Beach, SC, are also present in the microwave circuit in order to separate the three distinct voltage levels ($V_{\rm ID}$, V_H, and V_G). These capacitors provide a low-loss RF path in order to propagate the 5.8-GHz energy with little attenuation. When $V_{\rm ID} - V_G = 0$ V, the p-i-n diode has zero bias and is, therefore, in its off state reflecting the power incident upon it. When $V_{\rm ID} - V_G = 3$ V, the p-i-n is in its on state and passes the 5.8-GHz energy through its terminals. When the p-i-n is off, the measured insertion loss (isolation) for the RF circuit is 23 dB. When the p-i-n is on, the insertion loss is 1.5 dB. The RF circuit has a return loss better than 10 dB from 5 to 6.5 GHz when the p-i-n is on.

C. Digital Code

The microcontroller, which is powered by a 3-V input, outputs the 64-bit code shown in Fig. 8. This code is used to bias the p-i-n diode in order to modulate the 5.8-GHz carrier. The ID code is $6A7B49D20135FEC8_{16}$ = 0110 1010 0111 1011 0100 1001 1101 0010 0000 0001 0011 0101 1111 1110 1100 1000. This 64-bit code varies from 0 (off

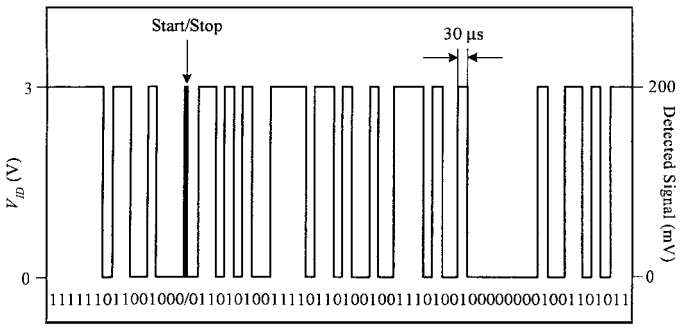

Fig. 8. Microcontroller output for biasing the p-i-n diode. The 64-bit code varies from $V_{\rm ID} = 0$ (off state) to $V_{\rm ID} = 3$ V (on state). Each bit takes 30 μs to process resulting in the 64-bit sequence taking 1.92 ms. ID code: $6A7B49D20135FEC8_{16} = 0110\,1010\,0111\,1011\,0100\,1001\,1101\,0010\,0000\,0001\,0011\,0101\,1111\,1110\,1100\,1000$.

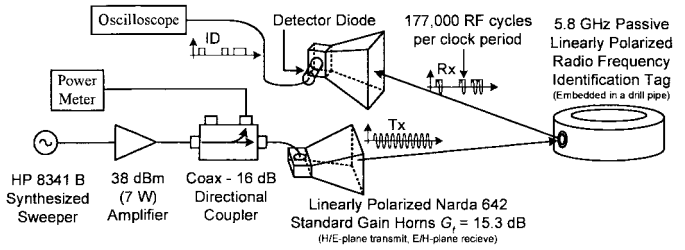

Fig. 9. RFID measurement setup. When the tag is oriented to receive energy from the horn in the H-plane, the receive horn should be E-plane oriented and vice versa.

state) to 3 V (on state). Each bit takes 30.5 μs to process resulting in the 64-bit sequence taking 1.952 ms.

D. Tag Free-Space Performance

For the free-space test of the tag illustrated in Fig. 9, a signal generator is used to provide microwave energy at various frequencies. This microwave energy is then fed to a 7-W amplifier in order to provide the necessary power to operate the tag's electronics. A horn then transmits the amplified signal to the tag, which is recessed into a cross-sectional slice of drill pipe. The tag's return signal is received by another horn rotated 90° with respect to the transmitting horn. This incoming signal is then detected by the reader with the use of a Schottky detector diode and displayed on an oscilloscope.

The system was successfully demonstrated in the laboratory for a distance of $x_2 = 30.5$ cm and a maximum transmit power of 7 W. The received demodulated code (detected signal) for broadside interrogation, i.e., $\theta_r = 0°$, $\phi_r = 0°$, and consequently, $\xi = 0°$ is shown in Fig. 8. A detector diode located on the receiving horn recovers the 64-bit code. The code has a 200-mV difference between its high and low levels. This difference results in the code being easily interpreted at the reader. The recovered code also matches the microcontroller's p-i-n diode biasing code indicating successful performance.

Fig. 10 presents the rectified voltage V_H versus frequency for different linearly polarized power densities incident upon the tag's 5-mm-thick Teflon surface when the distance $x_2 = 30.5$ cm. From Fig. 5, the 5-mm Teflon thickness will result in the resonant frequency 5.74 GHz. As expected, this is close

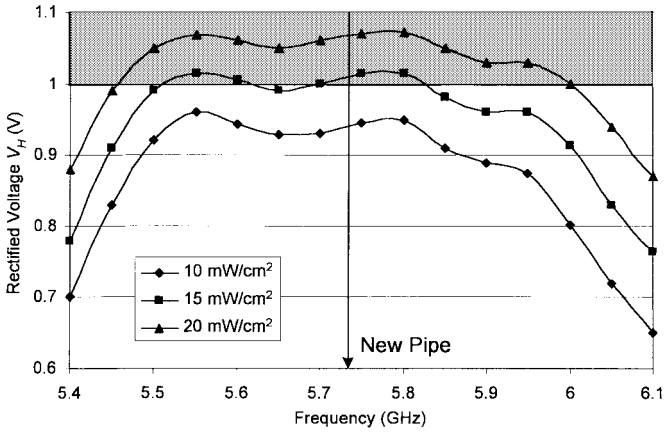

Fig. 10. Measured rectified voltage V_H versus frequency for different linearly polarized power densities incident upon the tag's Teflon surface. The Teflon thickness $t = 5$ mm corresponds to a new drill pipe. The shaded area reveals the voltage region ($V_H > 1$ V) when the tag's electronics are producing the 64-bit ID code. These curves are generated for broadside interrogation, i.e., $\theta_r = 0°$, $\phi_r = 0°$, and $\xi = 0°$.

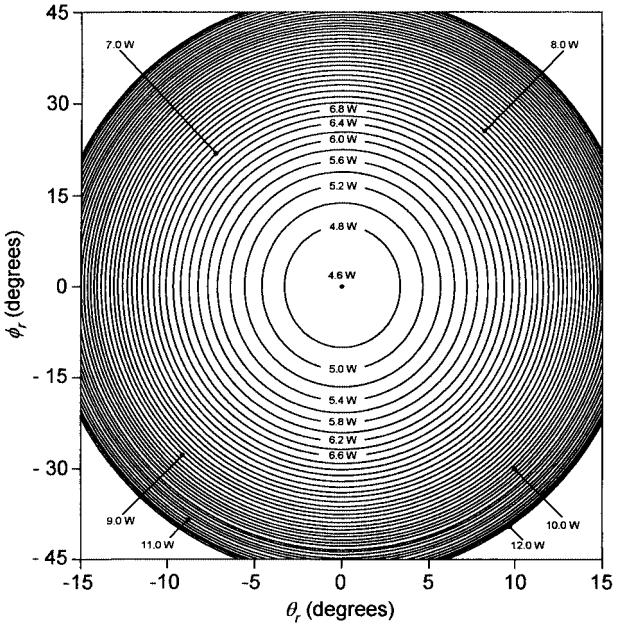

Fig. 11. Contour plot showing the transmit power needed to provide the 170 mW of 5.8-GHz energy to the Schottky rectifying diode for $x_2 = 1.0$ ft $\cong$ 30.5 cm. The angle ϕ_r varies from $-45°$ to 45°, and the angle θ_r ranges from $-15°$ to 15°.

to the center frequency of Fig. 10, as indicated by the vertical line. These curves are measured for broadside interrogation, i.e., $\theta_r = 0°$, $\phi_r = 0°$, and consequently, $\xi = 0°$. By applying these angles to (9) and (10) and inserting them into (2), the ratio of received to transmitted power becomes

$$\frac{P_r}{P_t} = (\lambda_o/4\pi x_2)^2\, 10^{15.3/10} 10^{8/10}. \tag{11}$$

The shaded area of Fig. 10 reveals the voltage region $V_H > 1$ V required for the tag's electronics to produce the 64-bit ID code. To turn on the tag at 5.8 GHz, a linearly polarized power density of approximately 13.5 mW/cm^2 is needed. The horn needs to transmit 4.6 W to achieve this power density when $x_2 = 1$ ft $= 30.5$ cm. Therefore, (11) reveals that the received power (P_r)

or the 5.8-GHz energy incident upon the Schottky diode needed to cause V_H to equal 1 V is approximately 170 mW.

Fig. 10 also reveals that the tag has broad-band performance due to the tag's recessed position in the drill pipe and broad-band matching caused by the diode and capacitor placements. For an incident linearly polarized power density of 20 mW/cm^2, the tag operates from 5.45 to 6 GHz. This broad-band performance is very important since mud films of varying thicknesses can cover the Teflon and shift the tag's resonant center frequency. With the additional bandwidth, the reader/tag link can be established at 5.8 GHz even with the thin mud film variations.

The contour plot of Fig. 11 predicts the transmit powers needed, based on (2), (9), and (10), to operate the tag for various θ_r's and ϕ_r's when $x_2 = 30.5$ cm. At this distance, $x_2 \gg d/2$ since most offshore drill pipe is 5 in in diameter. When $x_2 = 30.5$ cm, $\theta_r = 10°$, $\phi_r = 30°$, and consequently, $\xi = 31.5°$, the horn must transmit 9.3 W to get the 170 mW to the Schottky diode. This indicates that large transmit powers are necessary in maintaining the reader/tag link when the pipe is moving. This also justifies a need for low-power electronics [21], [22] and multiple reader antennas to interrogate at different positions around the pipe in order to reduce the transmit power levels. While high powers are readily available on the drilling platforms, being exposed to certain levels of it are a concern. Fortunately, personnel are normally at some distance away from the location of the reader's antenna, and a thick metal barrier will also separate the two.

IV. Conclusions

A new tag has been designed that has the potential of greatly reducing the operating costs of oil drilling and exploration. The passive tag is designed to operate without a battery and to withstand large pressures normal to its surface. The operational frequency 5.8 GHz allows for small size and a very high data rate to communicate multiple reads between the tag and reader. The tag's integration results in a wider bandwidth than a conventional patch antenna making it possible for the tag to operate when thin mud films of various thicknesses are present on the tag's Teflon surface.

Acknowledgment

The authors would like to thank M. Y. Li, Texas A&M University, College Station, and C. L. Wang, Texas A&M University, for fabricating the microstrip circuits and B. Roberson of Conroe, TX, for his assistance with the microcontroller programming. The authors would also like to acknowledge P. Koomey, Savage Koomey McDaniel Inc., Houston, TX, and G. Savage, Savage Koomey McDaniel Inc., Dallas, TX, for their insights from an oil industry perspective and their determination to facilitate such a design.

References

[1] P. Blythe, "RFID for road tolling, road-use pricing and vehicle access control," in *IEE RFID Technology Colloq.*, vol. 1, 1999, pp. 8/1–8/6.

[2] P. Hawkes, "Anti-collision and transponder selection methods for grouped 'vicinity' cards and PFID tags," in *IEE RFID Technology Colloq.*, vol. 1, 1999, pp. 7/1–7/12.

[3] M. Ollivier, "RFID—A new solution technology for security problems," in *Eur. Security and Detection Conv.*, 1995, pp. 234–238.

[4] A. Cerino and W. P. Walsh, "Research and application of radio frequency identification (RFID) technology to enhance aviation security," in *Nat. Aerospace and Electronics Conf.*, 2000, pp. 127–135.

[5] R. Hornby, "RFID solutions for the express parcel and airline baggage industry," in *IEE RFID Technology Colloq.*, vol. 1, 1999, pp. 2/1–2/5.

[6] T. Ruff and D. Hession-Kunz, "Application of radio-frequency identification systems to collision avoidance in metal/nonmetal mines," *IEEE Trans. Indus. Applicat.*, vol. 37, pp. 112–116, Jan./Feb. 2001.

[7] P. Record and W. Scanlon, "An identification tag for sea mammals," in *IEE RFID Technology Colloq.*, vol. 1, 1999, pp. 5/1–5/5.

[8] J. Sampaio, J. Placido, and S. Ferreira, "Radio-frequency-identification chips for drill string elements," *J. Petroleum Technol.*, pp. 47–48, Oct. 1998.

[9] C. W. Pobanz and T. Itoh, "Quasioptical microwave circuits for wireless applications," *Microwave J.*, pp. 64–85, Jan. 1995.

[10] C. W. Pobanz and T. Itoh, "A microwave noncontact identification transponder using subharmonic interrogation," *IEEE Trans. Microwave Theory Tech.*, vol. 43, pp. 1673–1679, July 1995.

[11] G. M. Savage, P. C. Koomey, and T. L. McDaniel, "System for drill string tallying tracking and service factor measurement," U.S. Patent 5 202 680, Apr. 13, 1993.

[12] J. O. McSpadden, L. Fan, and K. Chang, "Design and experiments of a high-conversion-efficiency 5.8-GHz rectenna," *IEEE Trans. Microwave Theory Tech.*, vol. 46, pp. 2053–2060, Dec. 1998.

[13] B. Strassner and K. Chang, "5.8 GHz circular polarized rectifying antenna for microwave power transmission," in *IEEE MTT-S Int. Microwave Symp. Dig.*, Phoenix, AZ, May 2001, pp. 1859–1862.

[14] T. Razban, R. Lemaitre, M. Bouthinon, and A. Coumes, "Passive transponder card system—Identifying objects through microwave interrogation," *Microwave J.*, pp. 135–146, Oct. 1987.

[15] L. Turner, "Passive electronic labels for remote object identification utilizing modulated RF backscatter," *J. Petroleum*, vol. 11, pp. 1–14, Apr. 1994.

[16] P. Salonen, M. Keskilammi, L. Sydanheimo, and M. Kivikoski, "An intelligent 2.45 GHz beam-scanning array for modern RFID reader," in *IEEE Int. Phased Array Systems and Techniques Conf.*, 2000, pp. 407–410.

[17] ——, "An intelligent 2.45 GHz multidimensional beam-scanning X-array for modern RFID reader," in *IEEE AP-S Int. Symp.*, vol. 1, 2000, pp. 190–193.

[18] K. F. Lee and W. Chen, *Advances in Microstrip and Printed Antennas*. New York: Wiley, 1997, pp. 165–177.

[19] K. Chang, *Microwave Solid-State Circuits and Applications*. New York: Wiley, 1994, pp. 208–218.

[20] C. Balanis, *Antenna Theory Analysis and Design*. New York: Wiley, 1982, pp. 64–65.

[21] D. Friedman, H. Heinrich, and D. Duan, "A low-power CMOS integrated circuit for field-powered radio frequency identification tags," in *IEEE Int. Solid-State Circuits Conf.*, 1997, pp. 294–295.

[22] U. Kaiser and W. Steinhagen, "A low-power transponder IC for high-performance identification systems," *IEEE J. Solid-State Circuits*, vol. 30, pp. 306–310, Mar. 1995.

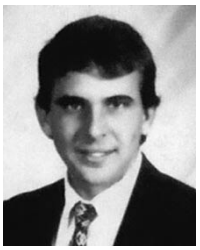

Berndie Strassner (S'96) received the B.S. degree in electrical engineering from the Rose-Hulman Institute of Technology, Terre Haute, IN, in 1995, and the M.S. and Ph.D. degrees in electrical engineering from Texas A&M University, College Station, TX, in 1997.

During the summer of 1992, 1993, and 1995, he was with the Johnson Space Center, Lockheed-Martin, where he was involved in the areas of space-shuttle navigational controls, power systems, and communication systems, respectively. In 1994, he was involved with microwave deembedding processes at the Technische Universität Hamburg-Harburg, Harburg, Germany. From 1996 to 1997, he was with Sandia National Laboratories, where he was involved with the study of the effects of harmonic termination on power-amplifier performance. From 1998 to 2002, he was a Research Assistant with the Electromagnetics Laboratory, Texas A&M University, where his research focused on RFID tags, rectifying antenna arrays, reflecting antenna arrays, and retro-directive antenna arrays. He is currently with Sandia National Laboratories, Albuquerque, NM, where he is involved with synthetic aperture radar for weapon guidance systems.

Kai Chang (S'75–M'76–SM'85–F'91) received the B.S.E.E. degree from the National Taiwan University, Taipei, Taiwan, R.O.C., in 1970, the M.S. degree from the State University of New York at Stony Brook, in 1972, and the Ph.D. degree from The University of Michigan at Ann Arbor, in 1976.

From 1972 to 1976, he was with the Microwave Solid-State Circuits Group, Cooley Electronics Laboratory, The University of Michigan at Ann Arbor, where he was a Research Assistant. From 1976 to 1978, he was with Shared Applications Inc., Ann Arbor, MI, where he was involved with computer simulation of microwave circuits and microwave tubes. From 1978 to 1981, he was with the Electron Dynamics Division, Hughes Aircraft Company, Torrance, CA, where he was involved in the research and development of millimeter-wave solid-state devices and circuits, power combiners, oscillators, and transmitters. From 1981 to 1985, he was with TRW Electronics and Defense, Redondo Beach, CA, where he was a Section Head involved with the development of state-of-the-art millimeter-wave integrated circuits and subsystems, including mixers, voltage-controlled oscillators (VCOs), transmitters, amplifiers, modulators, upconverters, switches, multipliers, receivers, and transceivers. In August 1985, he joined the Electrical Engineering Department, Texas A&M University, College Station, as an Associate Professor, and became a Professor in 1988. In January 1990, he became an E-Systems Endowed Professor of Electrical Engineering. He has authored and coauthored several books, including *Microwave Solid-State Circuits and Applications* (New York: Wiley, 1994), *Microwave Ring Circuits and Antennas* (New York: Wiley, 1996), *Integrated Active Antennas and Spatial Power Combining* (New York: Wiley, 1996), and *RF and Microwave Wireless Systems* (New York: Wiley, 2000). He has served as the Editor of the four-volume *Handbook of Microwave and Optical Components* (New York: Wiley, 1989 and 1990). He is the Editor of *Microwave and Optical Technology Letters* and the Wiley Book Series on "Microwave and Optical Engineering." He has also authored or coauthored over 350 technical papers and several book chapters in the areas of microwave and millimeter-wave devices, circuits, and antennas. His current interests are microwave and millimeter-wave devices and circuits, microwave integrated circuits, integrated antennas, wide-band and active antennas, phased arrays, microwave power transmission, and microwave optical interactions.

Dr. Chang was the recipient of the 1984 Special Achievement Award presented by TRW, the 1988 Halliburton Professor Award, the 1989 Distinguished Teaching Award, the 1992 Distinguished Research Award, and the 1996 Texas Engineering Experiment Station (TEES) Fellow Award presented by Texas A&M University.